

Self-trigger radio prototype array for GRAND

Yi Zhang,^{a,*} Haoning He^a and Pengfei Zhang^b on behalf of the GRAND Collaboration
(a complete list of authors can be found at the end of the proceedings)

^aKey Laboratory of Dark Matter and Space Astronomy, Purple Mountain Observatory,
Chinese Academy of Sciences, 210023 Nanjing, Jiangsu, China

^bXidian University,
266 Xinglong Section of Xifeng Road, 710126 Xian, Shaanxi, China
E-mail: zhangyi@pmo.ac.cn

The GRANDProto300 (GP300) array is a pathfinder for the Giant Radio Array for Neutrino Detection (GRAND) project. The deployment of the array, consisting of 300 antennas, will start in 2021 in a radio-quiet area of $\sim 200 \text{ km}^2$ near Lenghu ($\sim 3000 \text{ m a.s.l.}$) in China. Serving as a test bench, the GP300 array is expected to pioneer techniques of autonomous radio detection including identification and reconstruction of nearly horizontal cosmic-ray (CR) air showers. In addition, the GP300 array is at a privileged position to study the transition between Galactic and extragalactic origins of cosmic rays, due to its large effective area and the precise measurements of both energy and mass composition for CRs with energies ranging from 30 PeV to 1 EeV. Using the GP300 array we will also investigate the potential sensitivity for radio transients such as Giant Radio Pulses and Fast Radio Bursts in the 50-200 MHz range.

37th International Cosmic Ray Conference (ICRC 2021)
July 12th – 23rd, 2021
Online – Berlin, Germany

*Presenter

1. Introduction

The radio technique [1, 2] for detecting both cosmic rays and neutrinos at energies above around 100 PeV has matured. The Giant Radio Array for Neutrino Detection (GRAND)[3] will use a huge number of antennas to detect radio emission generated by extensive air showers (EASs) that are initiated by ultra-high-energy (UHE) particles in the atmosphere. GRAND will consist of roughly 20 separate, independent sub-arrays of approximately 10000 radio antennas each, totaling a combined area of 200000 km². GRAND is proposed as a large area observatory with unprecedented sensitivity for observations of UHE neutrinos, cosmic rays and gamma rays. It is expected to give revolutionary insights into the origin of UHE Cosmic Rays (CR) and the nature of UHE neutrino sources.

The GRANDProto300 (GP300) experiment is the 300-antenna pathfinder stage of GRAND. There are multiple goals for this stage. First of all, GP300 will validate GRAND as a standalone radio detection array and optimize the self-trigger techniques. Working as a self-triggering system can fully exploit the potential of the radio-detection technique. This is a challenge, as the background sources (high voltage power lines or transformers, planes, thunderstorms, etc.) dominate transient radio signals in the tens-of-MHz frequency range. Nevertheless, the principle for such a self-triggering mode for an EAS radio detector has been validated on a small-scale prototype array [4, 5]. In GP300, we will develop the algorithms to reject background and identify EAS events with improved efficiency.

Secondly, neutrino-induced EASs, which are of the major interest to GRAND, are near-horizontal, with zenith angles above $\sim 85^\circ$. GP300 will be an ideal test bench to improve the reconstruction algorithm for the direction, energy and air shower development, and evaluate the quality of the reconstruction procedure.

Finally, as the GP300 array will cover 200 km² and from its data we will be able to precisely measure the energy and mass composition for CRs from 30 PeV to 1 EeV, and to investigate the CR energy spectrum and anisotropy at the transition between Galactic and extragalactic origins of cosmic rays. The GP300 array will potentially also be sensitive to radio transients such as Giant Radio Pulses and Fast Radio Bursts at 50-200 MHz range.

2. The GP300 detector

The GP300 array, consisting of 300 detection units, covers a 200 km² radio-quiet area in the western part of China.

2.1 Deployment site and layout

The radio background noise level is an important factor for the autonomous radio detection for air showers. In our site-selection, we set the requirement that the integrated power of the stationary noise level would be less than twice the irreducible level due to Galactic and thermal ground emission in the 50-200 MHz. The other considerations are that there are no transient radio emission sources, around such as high-voltage power lines, windmills, etc.

We have started the site survey in August 2017, and several candidate sites have been visited in the Chinese provinces of Qinghai, Gansu, Xinjiang, Yunnan, and Inner-Mongolia. For two of

these sites we are now evaluating the ease of access, infrastructure, support by local authorities, and possible extension to the GRAND10k stage.

One candidate site close to the town of Lenghu in Qinghai Province was selected in July 2019. The long-term measurement facilities were deployed in the summer of 2019, to measure the time dependent behavior of the radio environment. Another candidate is in a natural preservation zone near Dunhuang in Gansu Province.

A data collection center is built at the site, as shown in Fig 1. The first 100 antennas of GP300 have been manufactured and tested, and will be installed at the site in summer 2021. The installation of the other 200 antennas is scheduled to be started in the middle of 2022.



Figure 1: A picture of the data collection center at the site.

The layout of GP300 covers an area of 200 km² with a regular grid using a 1 km antenna spacing, combined with a denser infill of 85 antennas with 500 m spacing and a core of 27 detectors on a 250 m grid.

2.2 Antennas

GRAND will detect radio signals from air showers initiated by Earth-skimming neutrinos, which arrive with zenith angles close to 90°. The GP300 antenna is designed to achieve a high detection efficiency for close to horizontal showers, therefore it is dubbed as the Horizontal Antenna. The height of the antennas is set to 3 m above ground to decrease the diffraction effect of radio waves off the ground.

Fig. 2 shows the schematic view of an antenna unit of GP300. The antenna unit is composed of 5 radiation arms. Two pairs of arms are symmetrical in the east-west and north-south directions, forming two horizontal linear polarization dipoles. The single arm in the vertical direction constitutes a monopole. The detector is operated at frequencies in the range of 50-200 MHz. The upper frequency will allow the detection of the radio Cherenkov-cone compared to previous experiments [4, 6–8]. As GP300 has a larger frequency range, a higher signal-to-noise ratio (SNR) and better reconstruction are expected [9].

2.3 DAQ

The analog signal in each antenna is first amplified by a 22dB low noise amplifier (LNA), and then sent over a 5 m cable to the main board where the signal is filtered in the 50-200 MHz

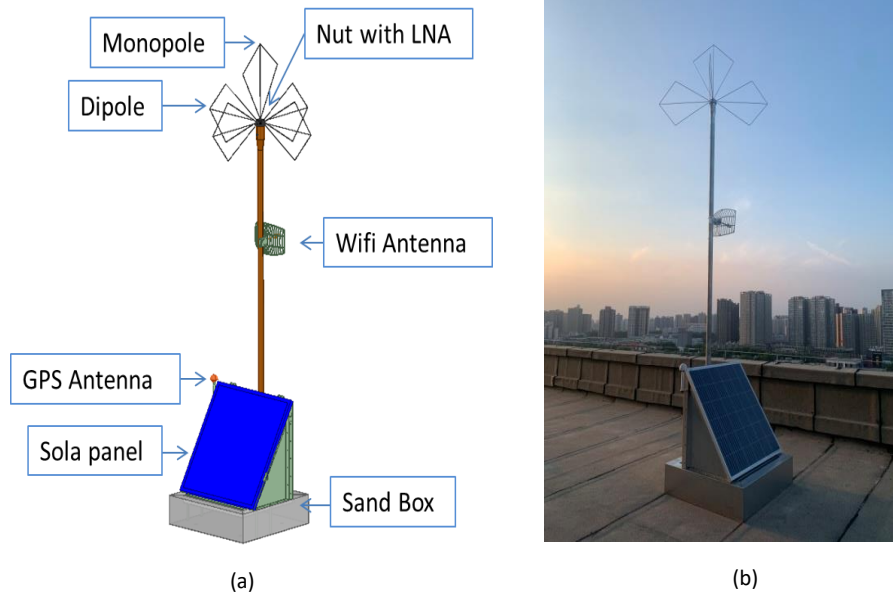


Figure 2: (a) Schematic view of the GP300 antenna unit. (b) Picture of a prototype.

frequency band and optionally amplified. Afterwards it is digitized using a 14-bit ADC (AD9694) running at a sampling rate of 500 Megasamples/s.

The digitized data is processed using a Zync FPGA with hardcore CPU (Xilinx XCZU5CG). Adjustable digital notch filters are used to reject continuous-wave emitters that may appear in this band. The FPGA will also process a real-time Fourier transform (FFT) of the data that can be used for the monitoring of radio background and searching for transient astronomical phenomena, such as FRBs.

We will transfer data to the central data acquisition (DAQ) room via WiFi technology, which allows for a throughput of 38 MB s^{-1} per sector of about 50 antennas, sufficient for our needs.

2.4 Trigger

We have designed three consecutive levels to progressively reduce the background:

- (T0) A zeroth-level trigger (T0) is generated for one antenna channel when the amplitude of a radio signal after filtering exceeds a threshold. The threshold is set at 5σ , where σ is the mean stationary noise at the antenna output.
- (T1) The first-level trigger (T1) performs a pulse shape analysis. It evaluates the duration and structure of the time traces, and the signal polarization. The algorithm based on pulse duration allows to reject 95% of the background events. T1 time-stamps are sent to the central DAQ for evaluation.
- (T2) The second-level trigger (T2) acts on the time-stamps sent by the T1 triggers and searches for time coincidences among a minimum of five detection neighboring antennas. If such a

detection is found, a 3 μ s-long time-trace from the T2-triggered detection units are transferred to the central DAQ.

In addition, there will be another mode to search for FRB-like transient radio waves. Each antenna will continuously calculate the FFT over 4096 samples in the 100 – 200 MHz frequency range (i.e. 25 kHz frequency resolution) and will sum them over periods of 10 ms.

2.5 Particle detector

A particle detector array with an independent trigger is planned in the GP300 phase. The particle detector array can both validate the horizontal reconstruction of radio signals, and have complementary measurements that enrich the physics of GP300. Either Water-Cherenkov detectors or scintillator detectors can be used in GP300, however the exact design and layout of the array requires a dedicated study. Even though these arrays are triggered independently, both particle detector array and radio array will be synchronized through GPS, so that their information can be combined to obtain the electromagnetic and muon components of air showers. In addition, we are investigating the option of adding FAST fluorescence telescopes [10] to the GP300 site.

3. Detector performances

GP300 will be twice as large as the current phase of Auger Engineering Radio Array [6]. The denser infill will improve the statistics of CRs at the energy down to about 30 PeV, while the large scale of the array, 200 km², makes it possible to derive sufficient statistics at the high energy end around 1 EeV. The different spacing between antennas allow to test the dependence of the array performance on the density of detection units. GP300 can detect about 10⁵ cosmic ray events in the energy range of 30 PeV-1 EeV after one-year operation, with an angular resolution better than 0.2°.

4. Science cases

4.1 Air shower physics

GP300 detector adopts the hybrid detection strategy to detect cosmic rays, by measuring the electromagnetic component via the radio array[7, 11] and the muon component via the ground array of particle detectors. From the measurement of the electromagnetic component, one can infer the depth of shower maximum and the energy of the primary cosmic ray[12], which is not sensitive to hadronic interaction models. The muon component together with the depth of shower maximum is correlated with the mass of the primary cosmic ray[13]. Therefore, with the measurements on electromagnetic component and muon component, we can test air-shower development for different hadronic interaction models.

4.2 Galactic/extra-galactic transition

GP300 is able to detect cosmic rays with energies beyond 30 PeV. It can detect about 100,000 cosmic ray events in the energy range of 30 PeV-1 EeV after one-year operation, and measure the energy and mass composition of cosmic rays more precisely[14]. Hence, GP300 is able to measure spectra of cosmic rays for each composition above the knee. It is widely believed that cosmic

rays below the knee originate mostly from Galactic sources, and a transition between Galactic and extra-galactic sources is expected in the energy range between 10^8 - 10^9 GeV[15]. Therefore, GP300's measurement of the spectra of cosmic rays for different compositions will help us to study the cause of the formation of the knee and the Galactic/extra-galactic transition, and furthermore, to constrain the astrophysical source models of cosmic rays.

4.3 Large scale anisotropy

GP300 is able to constrain the existence of a large scale Northern-Hemisphere anisotropy with an amplitude of 10^{-5} at the lower energy end[14], due to its large event statistics. The observation on the large scale of anisotropy will help us to constrain the existence of nearby UHECR sources. Besides the measurements of spectra and mass composition as mentioned in Section 4.2, the measurement of the large scale of anisotropy will give us one more tool to constrain the contributions from extra-galactic sources and Galactic sources, and then finally help us to study the Galactic/extra-galactic transition.

4.4 Ultra-high-energy gamma rays

Thanks to the particle detectors, the efficiency of distinguishing UHE gamma-rays from cosmic rays, for zenith angles between 65° and 85° above an energy of 10^9 GeV, is close to 100 %. If no gamma ray events are identified among a sample of 10^5 showers detected in 2 years, the fraction of gamma ray-initiated showers will be limited to be 0.03% at the 95% C.L., while the current best limit is about 0.14% at the energy of 10^9 GeV [16, 17]. The upper limit of UHE gamma-rays flux measured by GP300 would constrain the super heavy dark matter models [16]. If GP300 is triggered by a UHE gamma-ray-initiated shower, it would allow follow-up partner experiments in the multi-messenger network to search for counterparts associated with the triggered UHE gamma-ray.

4.5 Radio Astronomy

The GP300 sensitivity reaches 750 Jy in the band of 100-200 MHz, making Giant Pulses from the Crab [18] detectable. The large field of view and high duty-cycle allow GP300 to monitor the full sky for Fast Radio Burst(FRBs), Giant Pulses, searching for possible counterparts for Gravitational Wave Signals, and measuring of the 21-cm signature from the epoch of reionization (EoR).

5. Acknowledgements

This work is supported in China by the National Key R&D program of China under the grants 2018YFA0404202 and by the National Natural Science Foundation of China under the grants 11775233.

References

- [1] F. G. Schröder, Progress in Particle and Nuclear Physics **93**, 1 (2017), ISSN 0146-6410, URL <https://www.sciencedirect.com/science/article/pii/S0146641016300758>.

- [2] T. Huege and D. Besson, *Progress of Theoretical and Experimental Physics* **2017** (2017), ISSN 2050-3911, URL <http://academic.oup.com/ptep/article/doi/10.1093/ptep/ptx009/4665682>.
- [3] J. Álvarez Muñoz, R. Alves Batista, A. Balagopal V., J. Bolmont, M. Bustamante, W. Carvalho, D. Charrier, I. Cognard, V. Decoene, P. B. Denton, et al., *Science China Physics, Mechanics & Astronomy* **63**, 219501 (2019), ISSN 1869-1927, URL <https://doi.org/10.1007/s11433-018-9385-7>.
- [4] D. Ardouin, C. Cârloganu, D. Charrier, Q. Gou, H. Hu, L. Kai, P. Lautridou, O. Martineau-Huynh, V. Niess, O. Ravel, et al., *Astroparticle Physics* **34**, 717 (2011), ISSN 09276505, number: 9, URL <https://linkinghub.elsevier.com/retrieve/pii/S0927650511000041>.
- [5] D. Charrier, K. de Vries, Q. Gou, J. Gu, H. Hu, Y. Huang, S. Le Coz, O. Martineau-Huynh, V. Niess, T. Saugrin, et al., *Astroparticle Physics* **110**, 15 (2019), ISSN 0927-6505, URL <https://www.sciencedirect.com/science/article/pii/S0927650518302767>.
- [6] T. Huege (Pierre Auger), *Nucl. Instrum. Meth. A* **617**, 484 (2010), 0906.4970.
- [7] P. Schellart et al., *Astron. Astrophys.* **560**, A98 (2013), 1311.1399.
- [8] P. Bezyazeev, N. Budnev, O. Gress, A. Haungs, R. Hiller, T. Huege, Y. Kazarina, M. Kleifges, E. Konstantinov, E. Korosteleva, et al., *Nuclear Instruments and Methods in Physics Research Section A: Accelerators, Spectrometers, Detectors and Associated Equipment* **802**, 89 (2015), ISSN 0168-9002, URL <https://www.sciencedirect.com/science/article/pii/S0168900215010256>.
- [9] A. Balagopal V., A. Haungs, T. Huege, M. Renschler, F. G. Schröder, and A. Zilles, *PoS ICRC2019*, 184 (2020).
- [10] M. Malacari, J. Farmer, T. Fujii, J. Albury, J. Bellido, L. Chytka, P. Hamal, P. Horvath, M. Hrabovský, D. Mandat, et al., *Astroparticle Physics* **119**, 102430 (2020), ISSN 0927-6505, URL <https://www.sciencedirect.com/science/article/pii/S0927650520300037>.
- [11] T. Huege and Pierre Auger Collaboration, in *European Physical Journal Web of Conferences* (2019), vol. 210 of *European Physical Journal Web of Conferences*, p. 05011, 1905.04986.
- [12] A. Aab, P. Abreu, M. Aglietta, E. J. Ahn, I. Al Samarai, I. F. M. Albuquerque, I. Allekotte, P. Allison, A. Almela, J. Alvarez Castillo, et al., **116**, 241101 (2016), 1605.02564.
- [13] The Pierre Auger Collaboration, A. Aab, P. Abreu, M. Aglietta, E. J. Ahn, I. A. Samarai, I. F. M. Albuquerque, I. Allekotte, P. Allison, A. Almela, et al., arXiv e-prints arXiv:1604.03637 (2016), 1604.03637.
- [14] J. Álvarez-Muñoz, R. Alves Batista, A. Balagopal V., J. Bolmont, M. Bustamante, W. Carvalho, D. Charrier, I. Cognard, V. Decoene, P. B. Denton, et al., *Science China Physics, Mechanics, and Astronomy* **63**, 219501 (2020), 1810.09994.

- [15] B. R. Dawson, M. Fukushima, and P. Sokolsky, *Progress of Theoretical and Experimental Physics* **2017** (2017), [1703.07897](#).
- [16] A. Aab, P. Abreu, M. Aglietta, I. A. Samarai, I. F. M. Albuquerque, I. Allekotte, A. Almela, J. Alvarez Castillo, J. Alvarez-Muñiz, G. A. Anastasi, et al., **2017**, 009 (2017), [1612.01517](#).
- [17] A. Aab, P. Abreu, M. Aglietta, I. Al Samarai, I. F. M. Albuquerque, I. Allekotte, A. Almela, J. Alvarez Castillo, J. Alvarez-Muñiz, G. A. Anastasi, et al., **2020**, E02 (2020).
- [18] J. M. Cordes, N. D. R. Bhat, T. H. Hankins, M. A. McLaughlin, and J. Kern, **612**, 375 (2004), [astro-ph/0304495](#).

Full Authors List: GRAND Collaboration

Jaime Álvarez-Muñiz¹, Rafael Alves Batista², Aurélien Benoit-Lévy³, Julien Bolmont⁴, Henk Brans², Mauricio Bustamante⁵, Didier Charrier⁶, LingMei Cheng⁷, Simon Chiche⁸, Zigao Dai⁹, Rogerio M. de Almeida¹¹, Valentin Decoene¹², Peter B. Denton¹³, Beatriz de Errico¹⁴, Sijbrand De Jong^{2,15}, João R. T. de Mello Neto¹⁴, Krijn D. De Vries¹⁶, Kaikai Duan²¹, Ran Duan⁷, Ralph Engel^{17,18}, Yizhong Fan²¹, Ke Fang²², QuanBu Gou²³, Junhua Gu⁷, Claire Guépin^{19,20}, Jianhua Guo²¹, Yiqing Guo²³, Rene Habraken^{2,15}, Andreas Haungs¹⁷, Haoning He²¹, Eric Hivon⁸, Hongbo Hu²³, Xiaoyuan Huang²¹, Yan Huang⁷, Tim Huege^{17,10}, Marcelo Ismerio Oliveira¹⁴, Ramesh Koirala^{25,26}, Kumiko Kotera^{8,27}, Wen Jiang²⁴, Bruno L. Lago²⁸, Sandra Le Coz⁴, Jean-Philippe Lenain⁴, Bo Liu²⁴, Cheng Liu²³, Ruoyu Liu^{25,26}, Wei Liu²³, Pengxiong Ma²¹, Olivier Martineau-Huynh^{4,7,8}, Miguel Mostafá^{29,12}, Fabrice Mottez³⁰, Jean Mouette⁸, Kohta Murase^{29,12}, Valentin Niess³¹, Foteini Oikonomou³², Ziwei Ou³³, Tanguy Pierog¹⁷, Lech Wiktor Piotrowski³⁴, Simon Prunet³⁵, Xiangli Qian³⁶, Inge van Rens², Valentina Richard Romei⁸, Markus Roth¹⁷, Fabian Schüssler³⁷, Dániel Szálás-Motesiczky², Jikke Tacken², Anne Timmermans^{2,16}, Charles Timmermans^{2,15}, Matías Tüeros^{38,8}, Rongjuan Wang²⁴, Shen Wang²¹, Xiangyu Wang^{25,26}, Xu Wang³⁹, Clara Watanabe¹⁴, Daming Wei²¹, Feng Wei²⁴, Thei Wijnen², Xiangping Wu^{7,40}, Xuefeng Wu⁴¹, Xin Xu²⁴, Xing Xu²¹, Lili Yang³³, Xuan Yang²¹, Qiang Yuan²¹, Philippe Zarka⁴², Houdun Zeng²¹, Bing Theodore Zhang¹², Chao Zhang^{17,43,44}, Jianli Zhang⁷, Kewen Zhang⁴, Pengfei Zhang²⁴, Songbo Zhang⁴¹, Yi Zhang²¹, Hao Zhou⁴⁵

¹ Departamento de Física de Partículas & Instituto Galego de Física de Altas Enerxías, Universidad de Santiago de Compostela, 15782 Santiago de Compostela, Spain

² Institute for Mathematics, Astrophysics and Particle Physics (IMAPP), Radboud Universiteit, Nijmegen, Netherlands

³ Université Paris-Saclay, CEA, List, F-91120, Palaiseau, France

⁴ Sorbonne Université, Université Paris Diderot, Sorbonne Paris Cité, CNRS, Laboratoire de Physique Nucléaire et de Hautes Energies (LPNHE), 4 place Jussieu, F-75252, Paris Cedex 5, France

⁵ Niels Bohr International Academy, Niels Bohr Institute, 2100 Copenhagen, Denmark

⁶ SUBATECH, Institut Mines-Telecom Atlantique – CNRS/IN2P3 – Université de Nantes, Nantes, France

⁷ National Astronomical Observatories, Chinese Academy of Sciences, Beijing 100101, China

⁸ Sorbonne Université, CNRS, UMR 7095, Institut d'Astrophysique de Paris, 98 bis bd Arago, 75014 Paris, France

⁹ University of Science and Technology of China, 230026 Hefei, Anhui, China

¹⁰ Astrophysical Institute, Vrije Universiteit Brussel, Pleinlaan 2, 1050 Brussel, Belgium

¹¹ Universidade Federal Fluminense, EEIMVR, Volta Redonda, RJ, Brazil

¹² Department of Physics, Department of Astronomy & Astrophysics, Pennsylvania State University, University Park, PA 16802, USA

¹³ High Energy Theory Group, Physics Department, Brookhaven National Laboratory, Upton, NY 11973, USA

¹⁴ Universidade Federal do Rio de Janeiro (UFRJ), Instituto de Física, Brazil

¹⁵ Nationaal Instituut voor Kernfysica en Hoge Energie Fysica (Nikhef), Netherlands

¹⁶ IIHE/ELEM, Vrije Universiteit Brussel, Pleinlaan 2, 1050 Brussels, Belgium

¹⁷ Institute for Astroparticle Physics, Karlsruhe Institute of Technology (KIT), D-76021 Karlsruhe, Germany

¹⁸ Institute of Experimental Particle Physics (ETP), Karlsruhe Institute of Technology (KIT), D-76021 Karlsruhe, Germany

¹⁹ Department of Astronomy, University of Maryland, College Park, MD 20742-2421, USA

²⁰ Joint Space-Science Institute, College Park, MD 20742-2421, USA

- ²¹ Key Laboratory of Dark Matter and Space Astronomy, Purple Mountain Observatory, Chinese Academy of Sciences, 210023 Nanjing, Jiangsu, China
- ²² Wisconsin IceCube Particle Astrophysics Center (WIPAC) and Dept. of Physics, University of Wisconsin-Madison, Madison, WI 53703, USA
- ²³ Institute of High Energy Physics, Chinese Academy of Sciences, 19B YuquanLu, Beijing 100049, China
- ²⁴ Key Laboratory of Antennas and Microwave Technology, Xidian University, Xi'an 710071, China
- ²⁵ School of Astronomy and Space Science, Xianlin Road 163, Nanjing University, Nanjing 210023, China
- ²⁶ Key laboratory of Modern Astronomy and Astrophysics (Nanjing University), Ministry of Education, Nanjing 210023, People's Republic of China
- ²⁷ Vrije Universiteit Brussel (VUB), Dienst ELEM, Pleinlaan 2, B-1050, Brussels, Belgium
- ²⁸ Centro Federal de Educação Tecnológica Celso Suckow da Fonseca, Nova Friburgo, Brazil
- ²⁹ Center for Multimessenger Astrophysics, Pennsylvania State University, University Park, PA 16802, USA
- ³⁰ LUTH, Obs. de Paris, CNRS, Université Paris Diderot, PSL Research University, 5 place Jules Janssen, 92190 Meudon, France
- ³¹ Université Clermont Auvergne, CNRS/IN2P3, LPC, F-63000 Clermont-Ferrand, France.
- ³² Institutt for fysikk, NTNU, Trondheim, Norway
- ³³ School of Physics and Astronomy, Sun Yat-sen University, Zhuhai 519082, China
- ³⁴ Faculty of Physics, University of Warsaw, Pasteura 5, 02-093 Warsaw, Poland
- ³⁵ Laboratoire Lagrange, Université Côte d'Azur, Observatoire de la Côte d'Azur, CNRS, Parc Valrose, 06104 Nice Cedex 2, France
- ³⁶ Department of Mechanical and Electrical Engineering, Shandong Management University, Jinan 250357, China
- ³⁷ IRFU, CEA, Université Paris-Saclay, F-91191 Gif-sur-Yvette, France
- ³⁸ Instituto de Física La Plata, CONICET, Boulevard 120 y 63 (1900), La Plata, Argentina
- ³⁹ Department of Mechanical and Electrical Engineering, Shandong Management University, Jinan 250357, China.
- ⁴⁰ Shanghai Astronomical Observatory, Chinese Academy of Sciences, 80 Nandan Road, Shanghai 200030, China
- ⁴¹ Purple Mountain Observatory, Chinese Academy of Sciences, Nanjing 210023, China
- ⁴² LESIA, Observatoire de Paris, CNRS, PSL/SU/UPD/SPC, Place J. Janssen, 92195 Meudon, France
- ⁴³ Kavli Institute for Astronomy and Astrophysics, Peking University, Beijing 100871, China
- ⁴⁴ Department of Astronomy, School of Physics, Peking University, Beijing 100871, China
- ⁴⁵ Tsung-Dao Lee Institute & School of Physics and Astronomy, Shanghai Jiao Tong University, 200240 Shanghai, China